

# Performance Study of Multilayer Perceptrons in a Low-Cost Electronic Nose

Lei Zhang and Fengchun Tian

**Abstract**—Nonselective gas sensor array has different sensitivities to different chemicals in which each gas sensor will also produce different voltage signals when exposed to an analyte with different concentrations. Therefore, the characteristics of cross sensitivities and broad spectrum of nonselective chemical sensors promote the fast development of portable and low-cost electronic nose (E-nose). Simultaneous concentration estimation of multiple kinds of chemicals is always a challengeable task in E-nose. Multilayer perceptron (MLP) neural network, as one of the most popular pattern recognition algorithms in E-nose, has been studied further in this paper. Two structures of single multiple inputs multiple outputs (SMIMO) and multiple multiple inputs single output (MMISO)-based MLP with parameters optimization in neural network learning processing using eight computational intelligence optimization algorithms are presented in this paper for detection of six kinds of indoor air contaminants. Experiments prove that the performance in accuracy and convergence of MMISO structure-based MLP are much better than SMIMO structure in concentration estimation for more general use of E-nose.

**Index Terms**—Computational intelligence optimization, concentration estimation, electronic nose, indoor air contaminants, multilayer perceptron (MLP).

## I. INTRODUCTION

**E**LECTRONIC nose (E-nose) is an instrument embedded with a chemical sensor array [i.e., metal oxide semiconductor (MOS) gas sensors] of partial specificity and an appropriate pattern recognition algorithm used for detection of chemicals [1], [2]. In the past 20 years, a number of studies on E-nose have been presented for rapid detection and classification of chemicals in many fields, i.e., food industry [3]–[6], environmental monitor [7]–[9], medical diagnosis [10], [11], public security [12] and so on. Indoor air contaminants harm people's health quietly and a portable E-nose for monitoring the indoor air quality in real time is very necessary currently. Therefore, this paper aims for simultaneously quantification purposes of multiple kinds of indoor air contaminants by a portable E-nose.

Manuscript received July 9, 2013; revised October 25, 2013; accepted October 27, 2013. Date of publication January 24, 2014; date of current version June 5, 2014. This work was supported in part by the Hong Kong Scholar Program (No. XJ2013044) and in part by the New Academic Researcher Award for Doctoral Candidates granted by Ministry of Education in China. The Associate Editor coordinating the review process was Dr. Domenico Grimaldi.

L. Zhang is with the College of Computer Science, Chongqing University, Chongqing 400044, China, and also with The Hong Kong Polytechnic University, Hong Kong (e-mail: leizhang@cqu.edu.cn).

F. Tian is with the College of Communication Engineering, Chongqing University, Chongqing 400044, China.

Color versions of one or more of the figures in this paper are available online at <http://ieeexplore.ieee.org>.

Digital Object Identifier 10.1109/TIM.2014.2298691

Air contaminants reported in indoor air quality standard consist of four classes: physical, chemical, biological, and radioactive. Chemical contaminants including sulfur dioxide, nitrogen dioxide, carbon monoxide, carbon dioxide, ammonia, ozone, formaldehyde, benzene, toluene, inhalable particle, and volatile organic compounds were recognized as harmful substance to public health indoor [13]. This paper aims to detect six kinds of chemicals: formaldehyde, benzene, toluene, and ammonia exhausted from new furniture, oil paint, building materials of residuals, and carbon monoxide and nitrogen dioxide produced by the smoking of cigarettes, wood burning stoves, and car exhaust, which have been studied widely for their potential harms to people's health [13]–[15].

Artificial neural networks (ANNs), especially multilayer perceptrons (MLPs) based on back-propagation (BP) learning algorithm are one of the most popular pattern recognition (qualitative) and concentration estimation (quantitative) models in E-noses for environmental monitor applications, as remarked in [16]. The quantification models based on MLPs have been specially proposed for concentration estimation of pollutant gases [17]–[22]. In our previous research, we have also proposed the standardization model for sensor array's signal difference caused by new sensor replacement [23] and sensor drift prediction model [24] based on ANN.

There are two main facets of MLP to be discussed in E-nose for concentration estimation of multiple kinds of gases. The first thing is the parameters learning of MLP. MLP used in E-nose is generally trained by BP learning algorithm which has advantages of fast convergence and mean square error minimum. The second thing is the structure of MLP. Three layered MLP (input layer, one hidden layer, and output layer) is a satisfactory structure to solve a common regression problem in general. Therefore, the performance study of MLP in this paper is developed fully on the basis of these two facets. Particularly, two structures of single multiple inputs multiple outputs (SMIMO) and multiple multiple inputs single output (MMISO)-based MLP are studied for quantification of multiple kinds of indoor air contaminants.

Considering the disadvantage of easily trapped into local optimum of BP algorithm learned with initially random weights, we introduce eight computational intelligence optimization algorithms including standard genetic algorithm (SGA) [25], standard particle swarm optimization (SPSO) [26], IWA-PSO [27], ARPSO [28], DRPSO [29], PSOBC [30], and PSOAGS [18] for parameters optimization of MLP. In addition, we also introduce three linear regression methods including multivariate linear regression (MLR), partial least square (PLS) [31], [32], and prin-

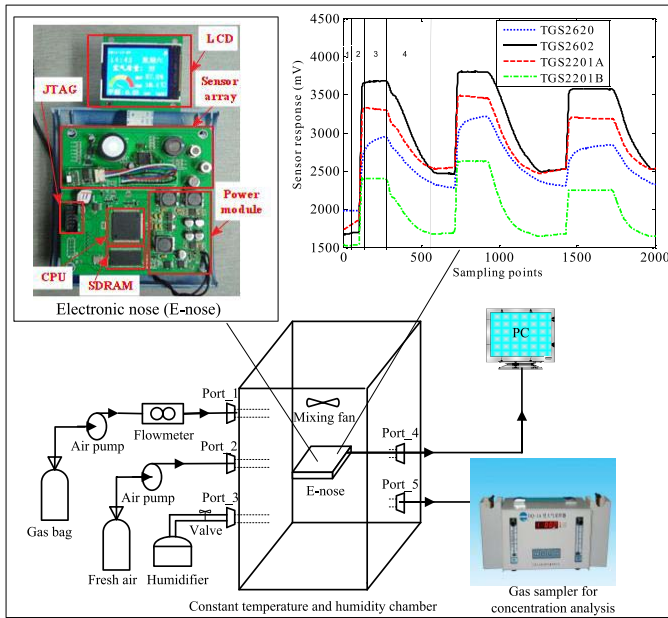


Fig. 1. Typical E-nose experimental platform.

principal component regression (PCR) [33], [34] which have been reported in E-nose system for concentration estimations and comparisons. The SMIMO-based MLP with parameters optimization has been studied in E-nose in our previous research [18]. This paper further employs the performance of MMISO-based MLP with parameters optimization in solution of a more complex problem and presents the comparison with SMIMO structure for more general use of a portable E-nose.

## II. EXPERIMENT

### A. Low-Cost E-Nose System Based on Sensor Array

The E-nose system has been introduced in our previous publications [9]. Consider the characteristics of cross sensitivity, broad spectrum response, and low cost of MOS gas sensors, our sensor array in E-nose system consists of only four MOS gas sensors manufactured in Figaro Inc. including TGS2602, TGS2620, TGS2201A, and TGS2201B. The heating voltage of TGS2620 and TGS2602 is 4 V, and the heating voltage of TGS2201A/B is 7 V. The supplied power voltage of system is dc12 V. In addition, considering that MOS gas sensors are sensitive to environmental temperature and humidity, a module (STD2230-I<sup>2</sup>C of Sensirion in Switzerland) with two auxiliary sensors for temperature ( $T$ ) and relative humidity (RH) measurement is also used in sensor array. A 12-b analog-digital converter is used as the interface between the field programmable gate array (FPGA) processor and the sensor array. FPGA is used for data collection, storage and processing in E-nose. The E-nose system is then connected to a personal computer (PC) via a joint test action group (JTAG) port which can be used for transferring data and debugging programs. The E-nose system and the experimental platform developed in our laboratory are shown in Fig. 1. The main components in the E-nose including the FPGA core CPU, SDRAM, JTAG, sensor array, power module, and LCD have been highlighted in Fig. 1. In addition, the typical response of an array of four

gas sensors to the first four phases in the sampling process [1] baseline; 2) transient response; 3) steady-state response; and 4) recover process] are also shown in Fig. 1.

### B. Experimental Setup

From the experimental platform shown in Fig. 1, the gaseous experiments of E-nose in this paper were employed in the constant temperature and humidity chamber (with type of LRH-150S), which can automatically adjust the temperature and humidity by setting up the target temperature and humidity in advance. The target gases were collected in a gas bag. The gas was injected to the chamber through a flowmeter. A fan is fixed in the chamber for purging, and the gas can diffuse evenly. In total, 10 min are consumed in each experiment and one sample is obtained. The specific experimental procedures including four stages can be generally illustrated as follows.

- 1) *Gas preparing and collection*: Collect each target gas in a bag, and dilute each target gas using pure nitrogen ( $N_2$ ).
- 2) *Data collection (major part)*: In this stage, there are several steps, shown as follows.
  - a) Step 1: Set the initial temperature and humidity of the chamber. For simulation of the indoor environment, 15, 20, 25, 30, and 35 °C are considered as target temperature, and 40%, 60%, and 80% are considered as target humidity. The specific combinations of temperature and humidity considered in the experiments are {(15, 60), (15, 80), (20, 40), (20, 60), (20, 80), (25, 40), (25, 60), (25, 80), (30, 40), (30, 60), (30, 80), (35, 60)}.
  - b) Step 2: Turn on the E-nose system until the temperature and humidity in the chamber reach the initial setting by authors, and then collect sensor array's responses of baseline for 2 min. Note that baseline denotes the initial state of sensor when exposed to clean air.
  - c) Step 3: Inject target gas by using a flowmeter with time controlled. Accordingly, turn on the gas sampler and it will keep 10 min sampling for true concentration analysis in this experiment. Then, the sensors will have quick response to target gas and until the sensors reach steady-state response after about 8 min. Therefore, one experiment of sample collection would sustain 10 min. The typical sensor response curves when exposed to each chemical of some concentration are shown in Fig. 2. The concentrations corresponding to the data shown in Fig. 2(a)–(f) are 0.18, 0.28, 0.14, 6.0, 0.5, and 1.62 ppm, respectively. Note that the paper focuses on the study of concentration estimation model, while the filtering and feature selection are not studied in deep. Therefore, the sensor response has been normalized within [0, 1] by dividing the maximum value (i.e.,  $x = x/x_{\max}$ ) for easier analysis of neural network. The steady-state response in Fig. 2 is extracted to represent the chemical feature for pattern analysis in a more effective way in actual application.

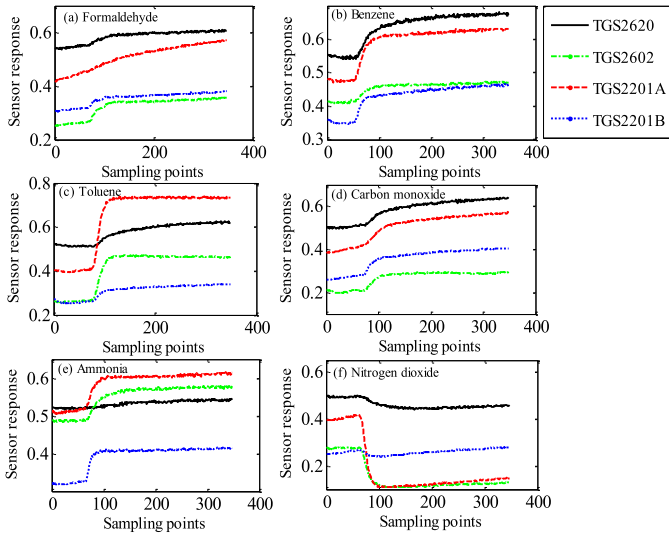


Fig. 2. Typical and normalized sensor response curves for six kinds of pollutant chemicals. (a) Formaldehyde. (b) Benzene. (c) Toluene. (d) Carbon monoxide. (e) Ammonia. (f) Nitrogen dioxide.

- 3) *Air exhaust and chamber cleaning*: After one experiment of sample collection, air exhaust by an air pump is necessary for chamber cleaning to recover the sensor to the initial state as soon as possible.
- 4) *Data transferring to PC*: Sensor response data in this experiment is obtained at this time through a JTAG connected between the E-nose and PC. Then the collected data can be transferred to the PC in a convenient way for data analysis and neural network learning in computer.

Finally, the learned results (i.e., hyper-parameters of neural networks) in computer would be transferred to the E-nose system for online detection of the target contaminants.

### C. E-Nose Data

Six kinds of indoor contaminants including formaldehyde ( $\text{CH}_2\text{O}$ ), benzene ( $\text{C}_6\text{H}_6$ ), toluene ( $\text{C}_7\text{H}_8$ ), carbon monoxide ( $\text{CO}$ ), ammonia ( $\text{NH}_3$ ), and nitrogen dioxide ( $\text{NO}_2$ ) have been studied in this paper. The E-nose experiments of each analyte are employed in terms of the illustrated experimental procedures. The specific information (i.e., target temperature, target humidity, and concentration) of each experimental sample for

each chemical has been presented in Table I. For instance, (15, 60) denotes the target temperature  $15^\circ\text{C}$  and RH 60%. In addition, the data statistics including the number of total samples, training samples, and testing samples, the lowest concentration (ppm) and the highest concentration (ppm) of each gas have been presented in Table II. Note that the approximated 2/3 training samples are randomly selected from the total samples of each gas for MLP learning.

### III. MLP-BASED QUANTIFICATION MODELS FOR MULTIPLE KINDS OF CHEMICALS

MLP neural network is used for learning on a large data set between sensor array data matrix  $\mathbf{P}$  and the target concentration **Target** using BP algorithm. The learned hyper-parameters are memorized in weights  $\mathbf{W}$  and bias  $\mathbf{B}$ . Then, the learned parameters of MLP are used for concentration estimation of unknown gas samples with a portable E-nose. Two structures (i.e., SMIMO and MMISO) for concentration estimation of six kinds of indoor contaminants are studied in this section.

#### A. SMIMO Model

SMIMO-based MLP model for concentration estimation of three kinds of chemicals has been studied in the previous research [18]. SMIMO is a straight forward method for prediction of multiple kinds of gases. Assume that the size of sensor array is  $m$  (number of sensors) and the number of chemicals in detection is  $q$ , then the number of input neurons and output neurons in SMIMO are also  $m$  and  $q$ , respectively. Namely, each output node represents a kind of gas. The structure of SMIMO-based MLP with one hidden layer is shown in Fig. 3(a).

The input training matrix  $\mathbf{P}$  and target concentration matrix **Target** of SMIMO for the training samples of all chemicals have been shown in (1), as shown at the bottom of the page, where each column in  $\mathbf{P}$  represents one feature vector corresponding to one observation sample,  $S_{i,j}$  ( $I = 1, \dots, m, j = 1, \dots, n_1 + n_2 + \dots + n_q$ ) is the extracted feature at the steady-state sensor response of each sample, and  $t_{1,k}$  ( $k = 1, \dots, n_1$ ),  $t_{2,k}$  ( $k = n_1 + 1, \dots, n_1 + n_2$ ),  $\dots$ ,  $t_{q,k}$  ( $k = n_1 + \dots + n_{q-1} + 1, \dots, n_1 + \dots + n_q$ ) are the target concentrations of gas\_1, gas\_2,  $\dots$ , gas\_ $q$ , respectively. Due to that the gas\_1, gas\_2,  $\dots$ , gas\_ $q$  are single gas in experiments, the target concentration vector

$$\begin{aligned}
 \mathbf{P} &= \begin{bmatrix} \overbrace{S_{1,1} S_{1,2} \cdots S_{1,n_1}}^{\text{gas}_1} & \overbrace{S_{1,n_1+1} S_{1,n_1+2} \cdots S_{1,n_1+n_2}}^{\text{gas}_2} & \cdots & \overbrace{S_{1,n_1+\dots+n_{q-1}+1} \cdots S_{1,n_1+\dots+n_q}}^{\text{gas}_q} \\ S_{2,1} S_{2,2} \cdots S_{2,n_1} & S_{2,n_1+1} S_{2,n_1+2} \cdots S_{2,n_1+n_2} & \cdots & S_{2,n_1+\dots+n_{q-1}+1} \cdots S_{2,n_1+\dots+n_q} \\ \vdots & \vdots & \vdots & \vdots \\ S_{m,1} S_{m,2} \cdots S_{m,n_1} & S_{m,n_1+1} S_{m,n_1+2} \cdots S_{m,n_1+n_2} & \cdots & S_{m,n_1+\dots+n_{q-1}+1} \cdots S_{m,n_1+\dots+n_q} \end{bmatrix} \\
 \mathbf{Target} &= \begin{bmatrix} \overbrace{t_{1,1} t_{1,2} \cdots t_{1,n_1}}^{\text{gas}_1} & \overbrace{0 \quad 0 \quad \cdots \quad 0}^{\text{gas}_2} & \cdots & \overbrace{0 \quad \cdots \quad 0}^{\text{gas}_q} \\ 0 \quad 0 \quad \cdots \quad 0 & \overbrace{t_{2,n_1+1} t_{2,n_1+2} \cdots t_{2,n_1+n_2}}^{\text{gas}_2} & \cdots & 0 \quad \cdots \quad 0 \\ \vdots & \vdots & \vdots & \vdots \\ 0 \quad 0 \quad \cdots \quad 0 & 0 \quad 0 \quad \cdots \quad 0 & \cdots & \overbrace{t_{q,n_1+\dots+n_{q-1}+1} \cdots t_{q,n_1+\dots+n_q}}^{\text{gas}_q} \end{bmatrix} \quad (1)
 \end{aligned}$$

TABLE I  
ELECTRONIC DATA OF INDOOR CONTAMINANTS EXPERIMENTS IN 12 CONDITIONS (T, RH)

Formaldehyde data (CH <sub>2</sub> O) (concentration unit: ppm)											
(15,60)	(15,80)	(20,40)	(20,60)	(20,80)	(25,40)	(25,60)	(25,80)	(30,40)	(30,60)	(30,80)	(35,60)
0.04	0.14	0.07	0.10	0.08	0.13	0.24	0.06	0.23	0.13	0.09	0.04
0.05	0.16	0.07	0.07	0.06	0.45	0.10	0.25	0.39	0.15	0.02	0.09
0.08	0.72	0.16	0.15	0.11	0.31	0.26	1.04	1.37	0.22	0.25	0.81
0.12	0.10	1.32	0.09	0.28	0.52	2.11	0.02	0.58	2.06	0.09	0.16
0.64	0.34	0.60	0.23	1.10	0.22	0.37	0.11	0.52	0.08	0.13	0.58
0.21	1.22	0.61	0.17	0.13	0.49	0.05	0.04	0.02	0.23	0.43	0.04
0.25	0.13	0.16	0.16	0.15	0.07	0.01	0.27	0.09	0.27	0.76	0.12
0.06	0.26	2.62	0.20	0.25	0.30	0.11	0.33	0.12	0.29	1.15	0.45
0.05	0.52	0.45	0.21	0.35	0.26	0.17	0.79	0.56	0.31	2.42	0.39
0.18	0.69	0.05	0.22	0.59	0.23	0.24	1.01	0.68	0.56	2.01	0.61
0.22	2.29	0.08	0.24	1.16	0.04	0.17	1.29	0.92	1.01	2.30	1.62
0.12	2.45	1.16	0.24	1.88	1.01	0.27	1.93	1.31	1.06		0.22
0.19	0.12	3.13	0.60	1.17	1.09	0.12	2.17	2.37	1.65		0.31
0.20	1.06	0.48	0.77	1.83	2.62	0.17	0.26	0.01	1.84		0.32
0.52	1.44	0.60	1.23		0.06	0.24	1.01	0.09	0.08		0.39
...	...	...	...		...	...	...	...	...		...
Benzene data (C <sub>6</sub> H <sub>6</sub> ) (concentration unit: ppm)											
(15,60)	(15,80)	(20,40)	(20,60)	(20,80)	(25,40)	(25,60)	(25,80)	(30,40)	(30,60)	(30,80)	(35,60)
0.17	0.17	0.17	0.17	0.17	0.17	0.17	0.17	0.17	0.17	0.17	0.17
0.28	0.28	0.28	0.28	0.28	0.28	0.28	0.28	0.28	0.28	0.28	0.28
0.49	0.49	0.49	0.49	0.49	0.49	0.49	0.49	0.49	0.49	0.49	0.49
0.91	0.91	0.91	0.91	0.91	0.91	0.91	0.91	0.91	0.91	0.91	0.91
0.71	0.71	0.71	0.71	0.71	0.71	0.71	0.71	0.71	0.71	0.71	0.71
0.11	0.06	0.09	0.08	0.20	0.19	0.15	0.15	0.19	0.15	0.20	0.14
0.18	0.20	0.07	0.15	0.06	0.10	0.13	0.06	0.18	0.18	0.13	
0.25	0.21	0.25	0.21	0.14	0.21	0.14	0.14	0.08	0.10	0.24	
0.18	0.11	0.26	0.36	0.16	0.18	0.19	0.16	0.24	0.19	0.22	
0.24	0.30	0.18	0.42	0.21	0.33	0.20	0.16	0.25	0.30		
0.32	0.22	0.06	0.43	0.21	0.16	0.10	0.20	0.18	0.41		
0.11	0.26	0.11				0.17	0.21	0.24			
Toluene data (C <sub>7</sub> H <sub>8</sub> ) (concentration unit: ppm)											
(15,60)	(15,80)	(20,40)	(20,60)	(20,80)	(25,40)	(25,60)	(25,80)	(30,40)	(30,60)	(30,80)	(35,60)
0.05	0.05	0.05	0.05	0.06	0.05	0.05	0.05	0.05	0.05	0.05	0.05
0.08	0.06	0.08	0.06	0.08	0.06	0.06	0.06	0.06	0.06	0.06	0.06
0.14	0.14	0.14	0.14	0.14	0.14	0.14	0.14	0.14	0.14	0.14	0.14
0.06	0.08	0.06	0.08	0.05	0.08	0.08	0.08	0.08	0.08	0.08	0.08
Carbon monoxide data (CO) (concentration unit: ppm)											
(15,60)	(15,80)	(20,40)	(20,60)	(20,80)	(25,40)	(25,60)	(25,80)	(30,40)	(30,60)	(30,80)	(35,60)
6	4	6	5	5	6	4	5	5	14	4	5
11	23	12	22	22	24	8	23	8	29	16	13
43	43	41	43	44	46	10	45	23	49	48	20
23	12	22	11	12	14	21	33	37	55	13	29
		13	9	20	10	12	48	6	25	16	20
Ammonia data (NH <sub>3</sub> ) (concentration unit: ppm)											
(15,60)	(15,80)	(20,40)	(20,60)	(20,80)	(25,40)	(25,60)	(25,80)	(30,40)	(30,60)	(30,80)	(35,60)
0.10	0.28	0.34	0.80	0.98	0.09	0.33	0.27	0.66	0.79	0.20	0.28
0.50		1.72	0.79	0.44	0.53	0.79	0.73	0.09	0.92	0.36	2.15
0.25		0.80			0.12	0.55			1.18		0.27
Nitrogen dioxide data (NO <sub>2</sub> ) (concentration unit: ppm)											
(15,60)	(15,80)	(20,40)	(20,60)	(20,80)	(25,40)	(25,60)	(25,80)	(30,40)	(30,60)	(30,80)	(35,60)
0.09		0.03	0.16	0.10	0.12	0.15	0.03		0.21		
0.20	-	0.92	0.84	0.54	0.31	0.22	0.05	-	0.61	-	-
1.62		0.77	0.28	0.18	0.20	0.70	0.87		1.36		
0.66						0.02	1.59				
							0.07				
							0.17				

of gas<sub>*i*</sub> in gas<sub>*j*</sub> ( $I = 1, \dots, q; j = 1, \dots, q; i \neq j$ ) should be **0** in the target concentration matrix **Target**.

Through the structure of SMIMO model, the neural network parameters learning are not flexible and difficult to be adjusted neatly with different kinds of gases due to that the prediction has been integrated in one single neural network.

*B. MMISO Model*

For further study, MMISO-based MLP model is an improvement of SMIMO model. In MMISO model, there are *q* single MLP neural networks for concentration estimation of *q* kinds of gases. The structure of MMISO with one hidden

TABLE II  
DATA STATISTICS OF EXPERIMENTAL SAMPLES EXPERIMENTS

Gases	$N_{total}$	$N_{training}$	$N_{testing}$	Lowest (ppm)	Highest (ppm)
CH <sub>2</sub> O	126	84	42	0.04	5.32
C <sub>6</sub> H <sub>6</sub>	72	50	22	0.17	0.91
C <sub>7</sub> H <sub>8</sub>	66	45	21	0.05	0.14
CO	58	42	16	5.00	49.0
NH <sub>3</sub>	29	20	9	0.09	2.15
NO <sub>2</sub>	30	20	10	0.03	1.62

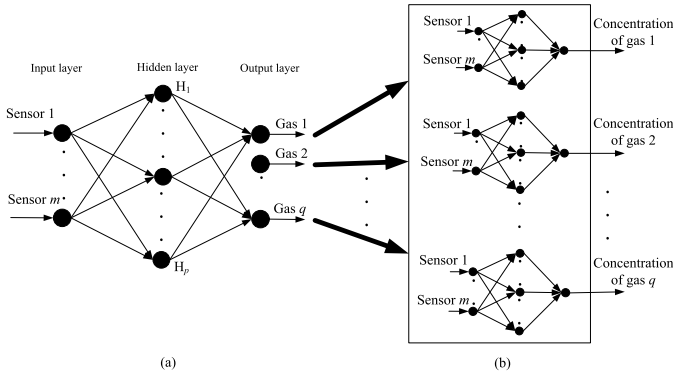


Fig. 3. Structures of (a) SMIMO- and (b) MMISO-based MLP concentration estimation models.

layer individually has been shown in Fig. 3(b). For each individual MLP (MLP<sub>1</sub>, MLP<sub>2</sub>, ..., MLP<sub>q</sub>),  $m$  input neurons and one output neuron are contained. The training data  $\mathbf{P}_{gas\_1}$ ,  $\mathbf{P}_{gas\_2}$ , ...,  $\mathbf{P}_{gas\_q}$  and the corresponding target concentration vectors  $\mathbf{Target}_{gas\_1}$ ,  $\mathbf{Target}_{gas\_2}$ , ...,  $\mathbf{Target}_{gas\_q}$  of MLP<sub>1</sub>, MLP<sub>2</sub>, ..., MLP<sub>q</sub> for quantification of gas<sub>1</sub>, gas<sub>2</sub>, ..., gas<sub>q</sub>, respectively, have been shown in

$$\left\{ \begin{array}{l}
 \mathbf{P}_{gas\_1} = \begin{bmatrix} S_{1,1}^{(1)} & S_{1,2}^{(1)} & \dots & S_{1,n_1}^{(1)} \\ S_{2,1}^{(1)} & S_{2,2}^{(1)} & \dots & S_{2,n_1}^{(1)} \\ \vdots & \vdots & \ddots & \vdots \\ S_{m,1}^{(1)} & S_{m,2}^{(1)} & \dots & S_{m,n_1}^{(1)} \end{bmatrix} \xRightarrow{\text{MLP}_1 \text{ learning}} \\
 \mathbf{Target}_{gas\_1} = [t_{1,1}^{(1)} \ t_{1,2}^{(1)} \ \dots \ t_{1,n_1}^{(1)}] \\
 \mathbf{P}_{gas\_2} = \begin{bmatrix} S_{1,1}^{(2)} & S_{1,2}^{(2)} & \dots & S_{1,n_2}^{(2)} \\ S_{2,1}^{(2)} & S_{2,2}^{(2)} & \dots & S_{2,n_2}^{(2)} \\ \vdots & \vdots & \ddots & \vdots \\ S_{m,1}^{(2)} & S_{m,2}^{(2)} & \dots & S_{m,n_2}^{(2)} \end{bmatrix} \xRightarrow{\text{MLP}_2 \text{ learning}} \\
 \mathbf{Target}_{gas\_2} = [t_{1,1}^{(2)} \ t_{1,2}^{(2)} \ \dots \ t_{1,n_2}^{(2)}] \\
 \vdots \\
 \mathbf{P}_{gas\_q} = \begin{bmatrix} S_{1,1}^{(q)} & S_{1,2}^{(q)} & \dots & S_{1,n_q}^{(q)} \\ S_{2,1}^{(q)} & S_{2,2}^{(q)} & \dots & S_{2,n_q}^{(q)} \\ \vdots & \vdots & \ddots & \vdots \\ S_{m,1}^{(q)} & S_{m,2}^{(q)} & \dots & S_{m,n_q}^{(q)} \end{bmatrix} \xRightarrow{\text{MLP}_q \text{ learning}} \\
 \mathbf{Target}_{gas\_q} = [t_{1,1}^{(q)} \ t_{1,2}^{(q)} \ \dots \ t_{1,n_q}^{(q)}]
 \end{array} \right. \quad (2)$$

where  $S_{i,j}^{(k)}$ ,  $i = 1, \dots, m$ ;  $j = 1, \dots, n_k$ ;  $k = 1, \dots, q$  in  $\mathbf{P}_{gas\_k}$  represents an extracted steady state feature in each sensor response of gas<sub>k</sub>, each column in  $\mathbf{P}_{gas\_k}$ ,  $k = 1, \dots, q$  represents a feature vector of one observation sample, and  $t_{i,j}^{(k)}$ ,  $i = 1, \dots, m$ ;  $j = 1, \dots, n_k$ ;  $k = 1, \dots, q$  is the corresponding target concentration of each column vector in  $\mathbf{P}_{gas\_k}$ .

Note that the MLP<sub>1</sub>, MLP<sub>2</sub>, ..., MLP<sub>q</sub> of each gas in MMISO model are learned individually and independently. The convergence performance (i.e., training goal, MSE) of MLP by BP training is also related with the training data and the target concentrations, while the target concentrations of each gas are also not in the same order of magnitude (i.e., the concentration ranges of CH<sub>2</sub>O, C<sub>6</sub>H<sub>6</sub>, C<sub>7</sub>H<sub>8</sub>, CO, NH<sub>3</sub> and NO<sub>2</sub> are within 0–6, 0.1–1, 0–0.2, 5–49, 0–3, and 0–2 ppm). Therefore, the MMISO model can be adjusted conveniently in terms of the characteristic of chemicals, avoid the disadvantages of SMIMO model, and improve the performance of convergence and prediction significantly.

### C. Parameters Optimization

BP neural network learning algorithm in this paper is the Levenberg–Marquardt (LM) algorithm [35], which takes the rule of mean square error minimum. LM is a fast algorithm with strong convergence ability and can get higher regression accuracy in learning of BP neural networks. LM algorithm is in fact a combination of Newton method and gradient descent. In addition, there is a special training function trainlm.m in MATLAB toolbox that we are using for convenient LM learning of the BP neural network. LM has been recognized as an effective learning algorithm in regression of this paper, but not that good in pattern recognition. However, the adjustments of hyper-parameters (i.e., weights and bias) are generally prone to premature convergence and trap into local optimum. Therefore, eight population-based intelligent optimization algorithms, i.e., genetic algorithm (GA), SPSO, inertia weight approach PSO (IWA-PSO), adaptive PSO (APSO), attractive and repulsive PSO (ARPSO), PSO based on diffusion and repulsion (DRPSO), PSO based on bacterial chemotaxis (PSOBC), and PSO based on adaptive genetic strategy (PSOAGS) have been studied generally for hyper-parameters optimization in this paper. Note that the computational intelligence optimizations can also not guarantee the global optimum theoretically. However, it can effectively improve the performance of convergence of BP neural network in engineering applications, promote the progress of E-nose accuracy in quantitative concentration estimation greatly, and satisfy the actual necessity.

Assume a structure  $m$ - $h$ - $o$  of MLP with three layers (input layer, one hidden layer, and output layer), then the weights matrix connected between the input layer and the hidden layer is  $\mathbf{W}_1$  ( $h \times p$ ), the bias vector of the hidden layer is  $\mathbf{B}_1$  ( $h \times 1$ ), the weights matrix connected between the hidden layer and the output layer is  $\mathbf{W}_2$  ( $o \times h$ ) and the bias vector of the output layer is  $\mathbf{B}_2$  ( $o \times 1$ ). The elements in weights and bias are viewed as genes in optimization, the weights and bias can be decoded

as a vector which is an individual in the population as follows:

$$\underbrace{x_1, x_2, \dots, x_{m \times h}}_{W_1}, \underbrace{x_{m \times h + 1}, \dots, x_{m \times h + h}}_{B_1} \quad (3)$$

$$\underbrace{x_{m \times h + h + 1}, \dots, x_{m \times h + h + o}}_{W_2}, \underbrace{x_{m \times h + h + o + 1}, \dots, x_L}_{B_2}$$

where  $m$ ,  $h$ , and  $o$  are the number of input neurons, hidden neurons, and output neurons, respectively. Therefore, the length  $L$  of an individual is  $L = m \times h + h + h \times o + o$ .

The cost function in the form of mean relative prediction error (MRPE, %) in optimization is illustrated as

$$\text{CostFun} = \max \left\{ \frac{1}{M_1} \sum_{i=1}^{M_1} \left| \frac{Y_i^{\text{tr}} - T_i^{\text{tr}}}{T_i^{\text{tr}}} \right|, \frac{1}{M_2} \sum_{j=1}^{M_2} \left| \frac{Y_j^{\text{te}} - T_j^{\text{te}}}{T_j^{\text{te}}} \right| \right\} \times 100 \quad (4)$$

where  $M_1$  denotes the number of training samples,  $M_2$  denotes the number of testing samples,  $\mathbf{Y}^{\text{tr}}$  and  $\mathbf{T}^{\text{tr}}$  represent the estimated and target concentrations of the training samples, and  $\mathbf{Y}^{\text{te}}$  and  $\mathbf{T}^{\text{te}}$  represent the estimated and target concentrations for the testing samples. The smaller value of *CostFun* corresponds to a lower MRPE and represents a better estimation performance.

In addition, the mean square error of prediction (MSEP, %) is also used for evaluation of the concentration estimation model. The MSEP in percentage can be represented as

$$\text{MSEP} = \frac{1}{M_2} \sum_{i=1}^{M_2} (Y_i^{\text{te}} - T_i^{\text{te}})^2 \times 100. \quad (5)$$

This paper studies the concentration estimation of six kinds of chemicals by portable E-noses. Therefore, in SMIMO structure-based MLP model, the network structure of SMIMO is set as 6–25–6 (six input neurons, 25 hidden neurons, and six output neurons). Six neural networks with the structure 6–10–1 are contained in MMISO.

For each computational intelligence optimization, the size  $M$  of population is set as 50 and the maximum generations  $G$  is set as 30 in experiments for equal comparison. The pseudocode implementation of the MMISO-based concentration estimation model with different computational intelligence optimization methods has been shown in Fig. 4.

#### IV. RESULTS AND DISCUSSION

In this paper, 12 methods including three linear methods (MLR, PLS, and PCR) and nine nonlinear methods (Single BP, SGA-BP, SPSO-BP, IWAPSO-BP, APSO-BP, DRPSO-BP, ARPSO-BP, PSOBC-BP, and PSOAGS-BP) often reported in E-nose are studied on concentration estimation of chemicals by an E-nose based on SMIMO and MMISO structures.

The MRPE of concentration estimation for indoor air contaminants based on SMIMO structure by using 12 methods have been presented in Table III. From Table III, the average MRPE of 139.7%, 195.4%, and 199.7% are obtained by using three linear methods, respectively, which demonstrate that linear

**Input:** Electronic nose data:  $\mathbf{P}_{\text{gas}_1}, \mathbf{P}_{\text{gas}_2}, \dots, \mathbf{P}_{\text{gas}_q}$ ;  $\mathbf{Target}_{\text{gas}_1}, \mathbf{Target}_{\text{gas}_2}, \dots, \mathbf{Target}_{\text{gas}_q}$ ;  
MLP: the number  $m$ ,  $h$  and  $o$  of input neurons, hidden neurons and output neurons, and MSE (training goal);  
Optimization: the length  $L$  of each individual, the population size  $M$ , and the maximum generations  $G$ ;  
(1) **switch** index  $(1, \dots, q)$  of gas  
(2) **case 1, do**  
determine the input matrix  $\mathbf{P}$  and output  $\mathbf{T}$  of MLP as  $\mathbf{P}_{\text{gas}_1}$  and  $\mathbf{Target}_{\text{gas}_1}$ ;  
**case 2, do**  
determine the input matrix  $\mathbf{P}$  and output  $\mathbf{T}$  of MLP as  $\mathbf{P}_{\text{gas}_2}$  and  $\mathbf{Target}_{\text{gas}_2}$ ;  
 $\vdots$   
**case  $q$ , do**  
determine the input matrix  $\mathbf{P}$  and output  $\mathbf{T}$  of MLP as  $\mathbf{P}_{\text{gas}_q}$  and  $\mathbf{Target}_{\text{gas}_q}$ ;  
(3) Randomly initialize the population and set  $Generation=0$ ;  
(4) **while**  $Generation < G$  **do**  
(5)  $Generation=Generation+1$ ;  
(6) **for**  $i=1$  to  $M$  **do**  
(7) Encode the individual as initial weights  $\mathbf{W}_1, \mathbf{W}_2$  and bias  $\mathbf{B}_1, \mathbf{B}_2$  according to Eq.(3);  
(8) Evaluates the individual through MLP training and calculate the cost function Eq.(4);  
(9) **end for**  
(10) Save the best individual from the population;  
(11) Update the population using one of the eight computational intelligence search algorithms.  
(12) **end while**;  
(13) Select the best individual from the total  $G$  generations  
(14) Encode the individual as initial weights  $\mathbf{W}_1, \mathbf{W}_2$  and bias  $\mathbf{B}_1, \mathbf{B}_2$  according to Eq.(3);  
(15) **end switch**

Fig. 4. Pseudocode implementation of the MMISO MLP-based concentration estimation model.

estimation methods are not qualified in our E-nose for indoor air contaminants detection.

The average MRPE of 76.13% is obtained by using nonlinear BP MLP neural network. Note that the results of single BP is obtained by running BP  $20 \times$  and calculate the average value of the  $20 \times$ , because the result of BP is not stable for every time. In addition, considering that single BP is easily trapped into local minimum, APSO-BP and PSOAGS-BP through the parameters optimization of neural network are the first two methods which have lowest average MRPE of 49.35% and 57.97%, respectively. The lowest MRPEs for prediction of formaldehyde, benzene, toluene, carbon monoxide, ammonia, and nitrogen dioxide are 77.74%, 33.83%, 56.18%, 15.14%, 46.73%, and 66.47%, respectively.

Table IV presents the MSEPs in percentage using 12 concentration estimation methods based on SMIMO structure. Due to the difference of computation between MRPE and MSEP, the MSEPs of formaldehyde, benzene, toluene, carbon monoxide, ammonia and nitrogen dioxide are 85.86%, 4.97%, 0.30%, 16.87, 8.99%, and 13.93% with APSO-BP method, and the average MSEP is 21.82% which has become much lower than the MRPE. However, in the measurement subject, MRPE is a preferred evaluation method, but not MSEP.

Though the estimation results of MRPE and MSEP illustrated in Tables III and IV have been largely improved by using nonlinear methods with parameters optimization gradually, the estimation performance of SMIMO-based model is still very

TABLE III  
MRPEs OF INDOOR CONTAMINANTS BASED ON SMIMO STRUCTURE EXPERIMENTS

Methods based on SMIMO structure	MRPE (%)						
	CH <sub>2</sub> O	C <sub>6</sub> H <sub>6</sub>	C <sub>7</sub> H <sub>8</sub>	CO	NH <sub>3</sub>	NO <sub>2</sub>	Average
MLR	197.9	169.1	164.1	42.45	74.88	189.6	139.7
PLS	412.0	131.2	334.9	45.98	93.37	154.6	195.4
PCR	252.7	116.6	451.1	105.0	81.08	191.4	199.7
Single BP	213.2	34.04	37.76	30.59	63.58	77.61	76.13
SGA-BP	111.7	33.85	39.60	34.06	77.08	68.82	60.13
SPSO-BP	104.2	38.38	61.05	37.99	66.74	70.05	63.06
IWAPSO-BP	94.70	41.09	53.76	50.96	64.16	75.44	63.35
APSO-BP	77.74	33.83	56.18	15.14	46.73	66.47	<b>49.35</b>
DRPSO-BP	92.16	40.87	41.14	38.41	69.39	73.46	59.24
ARPSO-BP	61.39	51.05	75.31	39.59	77.78	83.28	64.73
PSOBC-BP	106.1	29.53	50.48	33.98	71.78	67.87	60.67
PSOAGS-BP	105.9	32.14	27.12	38.43	74.42	69.79	<b>57.97</b>

TABLE IV  
MSEPs FOR INDOOR CONTAMINANTS CONCENTRATION ESTIMATION BASED ON SMIMO STRUCTURE EXPERIMENTS

Methods based on SMIMO structure	MSEP (%)						
	CH <sub>2</sub> O	C <sub>6</sub> H <sub>6</sub>	C <sub>7</sub> H <sub>8</sub>	CO	NH <sub>3</sub>	NO <sub>2</sub>	Average
MLR	556.4	124.1	2.600	132.6	23.08	113.4	158.7
PLS	2411	74.75	10.84	155.6	35.89	75.37	460.7
PCR	907.3	59.04	19.66	811.2	27.06	115.3	323.3
Single BP	645.8	5.030	0.140	68.85	16.64	19.00	125.9
SGA-BP	177.3	4.980	0.150	85.36	24.46	14.94	51.19
SPSO-BP	154.3	6.400	0.360	106.2	18.34	15.47	50.17
IWAPSO-BP	127.4	7.330	0.280	191.1	16.95	17.95	60.17
APSO-BP	85.86	4.970	0.300	16.87	8.990	13.93	21.82
DRPSO-BP	120.7	7.250	0.160	108.6	19.82	17.02	45.58
ARPSO-BP	53.54	11.32	0.550	115.3	24.90	21.87	37.92
PSOBC-BP	159.9	3.790	0.250	84.96	21.21	14.53	47.44
PSOAGS-BP	159.3	4.490	0.070	108.7	22.80	15.36	51.78

weak for detection of multiple kinds of indoor contaminants by an E-nose.

Therefore, the MMISO model is presented for improvement of the E-nose detection. The estimation results MRPE of E-nose have been presented in Table V. The first two methods with the lowest average MRPE of 23.13% and 23.54% are obtained using PSOAGS-BP and PSOBC-BP based on MMISO model. The lowest MRPEs for prediction of formaldehyde, benzene, toluene, carbon monoxide, ammonia, and nitrogen dioxide are 30.55%, 6.587%, 16.15%, 6.115%, 31.41%, and 47.95%, respectively. Through the results of Table V, we can find that the estimation performance of MMISO has been improved significantly than SMIMO-based model.

Table VI presents the concentration estimation analysis using the evaluation of MSEP in percentage based on MMISO structure. The MSEP of PSOAGS-BP method for formaldehyde, benzene, toluene, carbon monoxide, ammonia, and nitrogen dioxide are 7.10%, 0.26%, 0.033%, 3.09%, 4.30%, and 5.58%, respectively. The lowest average MSEPs are 3.33% and 3.45% obtained by PSOBC-BP and PSOAGS-BP, which have significant improvement than SMIMO-based structure. The results from Tables V and VI

demonstrate that the proposed MMISO-based structure is very effective for concentration estimation of multiple kinds of indoor air contaminants.

For directly perceived through the senses, we have presented the performance comparisons of SMIMO and MMISO models using 12 estimation methods in Fig. 5. Fig. 5(a)–(f) illustrates the estimation MRPEs of formaldehyde, benzene, toluene, carbon monoxide, ammonia, and nitrogen dioxide, respectively, using 12 methods. [Index of methods in the horizontal axis of each subfigure: 1) MLR; 2) PLS; 3) PCR; 4) single BP; 5) SGA-BP; 6) SPSO-BP; 7) IWAPSO-BP; 8) APSO-BP; 9) DRPSO-BP; 10) ARPSO-BP; 11) PSOBC-BP; and 12) PSOAGS-BP]. It is clear that the MRPE of estimation for each gas of MMISO is much lower than SMIMO structure-based MLP model using nonlinear estimation methods. This demonstrates that the MMISO is much better than SMIMO structure in detection of multiple kinds of gases by portable E-noses due to that cross errors have been occurred in SMIMO during the learning process due to the correlation among sensor signals.

It is worth noting that the though the MRPEs of estimation seems to be still large in measurement by using the proposed method, while the results of this paper are actual experimen-

TABLE V  
MRPEs OF INDOOR CONTAMINANTS USING MMISO-BASED STRUCTURE EXPERIMENTS

Methods based on MMISO structure	MRPE (%)						
	CH <sub>2</sub> O	C <sub>6</sub> H <sub>6</sub>	C <sub>7</sub> H <sub>8</sub>	CO	NH <sub>3</sub>	NO <sub>2</sub>	Average
MLR	258.8	10.07	20.82	18.56	70.99	80.67	76.65
PLS	330.1	21.93	22.31	50.03	94.84	122.7	106.9
PCR	372.7	104.1	95.69	122.9	129.1	154.9	163.2
Single BP	158.7	15.51	65.56	17.67	120.5	77.61	75.93
SGA-BP	34.25	7.270	18.71	6.264	44.06	60.98	28.59
SPSO-BP	32.36	6.935	18.71	5.103	29.43	54.70	24.54
IWAPSO-BP	32.67	7.323	17.63	7.651	47.79	69.69	30.46
APSO-BP	31.66	5.679	18.01	6.539	34.12	65.59	26.93
DRPSO-BP	31.38	7.196	17.95	6.677	35.40	60.71	26.55
ARPSO-BP	31.56	6.879	17.16	7.377	38.32	63.41	27.45
PSOBC-BP	31.18	6.951	17.83	6.426	28.11	50.79	<b>23.54</b>
PSOAGS-BP	30.55	6.587	16.15	6.115	31.41	47.95	<b>23.13</b>

TABLE VI  
MSEPs FOR INDOOR CONTAMINANTS CONCENTRATION ESTIMATION USING MMISO-BASED STRUCTURE EXPERIMENTS

Methods based on MMISO structure	MSEP (%)						
	CH <sub>2</sub> O	C <sub>6</sub> H <sub>6</sub>	C <sub>7</sub> H <sub>8</sub>	CO	NH <sub>3</sub>	NO <sub>2</sub>	Average
MLR	825.6	0.430	0.430	26.56	15.90	20.69	148.3
PLS	1350	1.920	0.470	183.9	28.46	46.94	268.6
PCR	1716	46.97	0.870	1095	52.48	74.79	497.7
Single BP	120.7	0.950	0.475	24.00	85.31	68.92	50.06
SGA-BP	10.61	0.390	0.081	3.39	7.62	10.03	5.353
SPSO-BP	11.23	0.330	0.052	3.450	16.31	4.46	5.972
IWAPSO-BP	11.26	0.320	0.041	4.320	11.27	13.18	6.732
APSO-BP	9.750	0.270	0.044	2.180	4.660	9.35	4.376
DRPSO-BP	10.05	0.410	0.042	3.020	14.38	8.78	6.114
ARPSO-BP	19.15	0.300	0.034	2.080	6.170	8.030	5.961
PSOBC-BP	10.59	0.340	0.033	2.130	4.890	1.980	<b>3.327</b>
PSOAGS-BP	7.710	0.260	0.033	3.090	4.030	5.580	<b>3.451</b>

TABLE VII  
TIME CONSUMPTION FOR RUNNING ALL ALGORITHMS EXPERIMENTS

Model	Time consumption for running all algorithms in computer (unit: hour)						
	CH <sub>2</sub> O	C <sub>6</sub> H <sub>6</sub>	C <sub>7</sub> H <sub>8</sub>	CO	NH <sub>3</sub>	NO <sub>2</sub>	Total time
SMIMO	-	-	-	-	-	-	27.0
MMISO	2.94	0.54	0.32	3.22	1.75	1.15	9.90

tal test, the seemingly large error results from the E-nose system and experimental data. Currently, the E-nose system is developed based on a MOS gas sensor array which has characteristic of low cost and broad spectrum but low accuracy. The cross sensitivity of MOS gas sensors combined with pattern recognition can make E-nose detect multiple kinds of contaminants. Generally, the E-nose with one electrochemical gas sensor developed in our lab has a high accuracy in measurement of formaldehyde concentration. The MRPE is around 20% for electrochemical sensor, but it can only be used for formaldehyde test. The defect of E-nose based on electrochemical sensor is the single gas detection and higher cost. In addition, the experimental data is also an aspect

in the estimation performance. In this paper, we have used all the data without any possible outlier or noise removal for analysis, considering that the robustness (generality of prediction) is also important in detection. A good accuracy in computer cannot guarantee a successful prediction in actual application due to the complex environmental conditions. Instead, the existence of noise in the learning data set can enhance the ability of noise-counteraction in an E-nose. In addition, the disadvantage of easily trapped into local minimum for BP neural network can be improved by the intelligent optimizations which have been significant in E-nose detection from the presented results, though the computational intelligence optimizations can also not guarantee the seriously

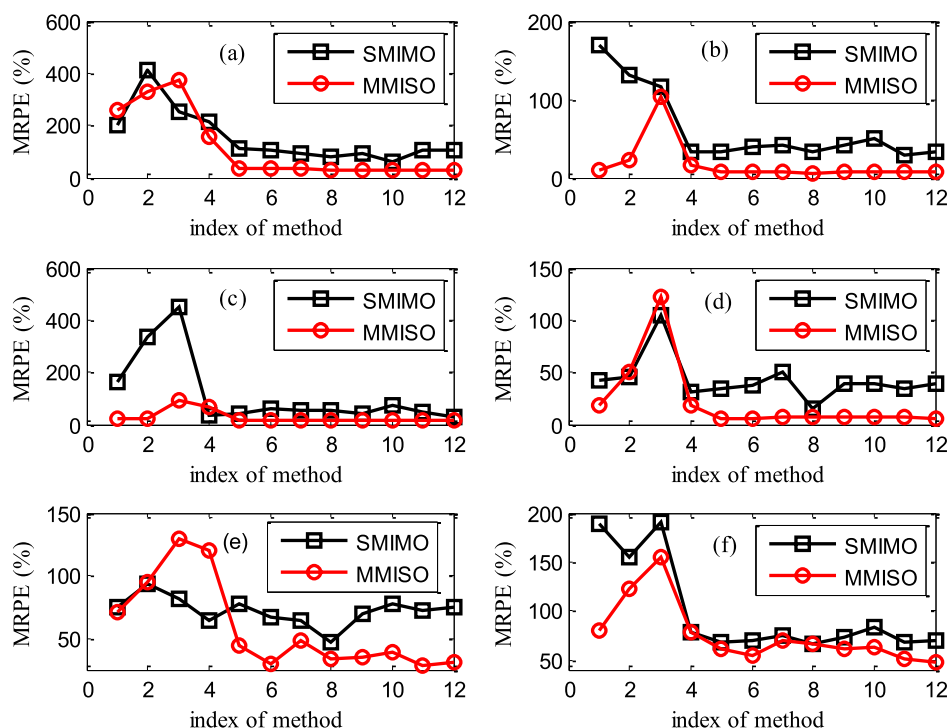


Fig. 5. Estimation performance comparisons of SMIMO and MMISO structure using 12 methods. Index of methods: (1) MLR, (2) PLS, (3) PCR, (4) single BP, (5) SGA-BP, (6) SPSO-BP, (7) IWAPSO-BP, (8) APSO-BP, (9) DRPSO-BP, (10) ARPSO-BP, (11) PSOBC-BP, and (12) PSOAGS-BP. Prediction of chemicals: (a) formaldehyde, (b) benzene, (c) toluene, (d) carbon monoxide, (e) ammonia, and (f) nitrogen dioxide.

global optimum theoretically. Therefore, we can say that the estimation performance in this paper can be accepted with an average MRPE of 23% and an average MSEP of 3%.

On the other hand, the time consumptions of SMIMO and MMISO for running all the estimation algorithms for each gas have been also shown in Table VII for comparing their efficiency in application. Due to that SMIMO realize the estimation of each gas at the same time and the SMIMO model endures a larger burden for MLP training because of larger data set which consists of all training data, the total time for SMIMO is calculated as approximately 27 h. Due to that the estimation of each gas is independent based on the MMISO structure, 2.94, 0.54, 0.32, 3.22, 1.75, and 1.15 h are consumed for parameters learning of formaldehyde, benzene, toluene, carbon monoxide, ammonia, and nitrogen dioxide, respectively. Totally, 9.9 h are consumed for all chemicals based on MMISO. Therefore, it is clear that the efficiency of MMISO is also much higher than SMIMO. The estimation performance and efficiency fully prove that MMISO model is a better selection for concentration estimation of multiple kinds of gases in E-nose development.

Note that the running time shown in Table VII is only for algorithm learning in computer, but not in E-nose system, considering the higher cost of CPU and the real-time characteristic in an E-nose. The learned results (i.e., the weights of neural network) will be transferred to the E-nose system, and perform the feed-forward computation of MLP instead. The computation velocity is in the level of microsecond ( $\mu$ s), and therefore, it can still promise the real-time characteristic of E-nose detection.

## V. CONCLUSION

This paper presents a performance study of SMIMO and MMISO-based MLP with parameters optimization for quantifying the concentration of six kinds of indoor air contaminants by a portable E-nose. There are three major findings in experiments that concentration estimation of multiple kinds of chemicals by an E-nose with nonselective chemical sensors is a completely nonlinear problem when compared with those three linear methods, computational intelligence optimizations are very effective in improving the parameters learning of MLP based on BP algorithm, and MMISO structure-based MLP has better superiorities for quantifying multiple kinds of chemicals than SMIMO in terms of the estimation accuracy and the time consumption of algorithm convergence.

## ACKNOWLEDGMENT

The authors would like to thank the Bureau of Standard Measurement for their valuable assistance. The authors would also like to express their sincere appreciation to the anonymous reviewers for their insightful comments, which have greatly improved the quality of this paper.

## REFERENCES

- [1] J. W. Gardner and P. N. Bartlett, *Electronic Noses: Principles and Applications*. London, U.K.: Oxford Univ. Press, 1999.
- [2] S. M. Scott, D. James, and Z. Ali, "Data analysis for electronic nose systems," *Microchimica Acta*, vol. 156, no. 3, pp. 183–207, 2006.
- [3] K. Brudzewski, S. Osowski, and A. Dwulit, "Recognition of coffee using differential electronic nose," *IEEE Trans. Instrum. Meas.*, vol. 61, no. 6, pp. 1803–1810, Jun. 2012.

- [4] S. Osowski, T. H. Linh, and K. Brudzewski, "Neuro-fuzzy network for flavor recognition and classification," *IEEE Trans. Instrum. Meas.*, vol. 53, no. 3, pp. 638–644, Jun. 2004.
- [5] N. Bhattacharyya, R. Bandyopadhyay, M. Bhuyan, B. Tudu, D. Ghosh, and A. Jana, "Electronic nose for black tea classification and correlation of measurement with "Tea Taster" marks," *IEEE Trans. Instrum. Meas.*, vol. 57, no. 7, pp. 1313–1321, Jul. 2008.
- [6] B. Tudu, A. Metla, B. Das, N. Bhattacharyya, A. Jana, D. Ghosh, *et al.*, "Towards versatile electronic nose pattern classifier for black tea quality evaluation: An incremental fuzzy approach," *IEEE Trans. Instrum. Meas.*, vol. 58, no. 9, pp. 3069–3078, Sep. 2009.
- [7] E. Llobet, J. Brezmes, R. Ionescu, X. Vilanova, S. Al-Khalifa, J. W. Gardner, *et al.*, "Wavelet transform and fuzzy ARTMAP-based pattern recognition for fast gas identification using a micro-hotplate gas sensor," *Sensors Actuat. B, Chem.*, vol. 83, nos. 1–3, pp. 238–244, 2002.
- [8] M. Shi, A. Bermak, S. B. Belhouari, and P. C. H. Chan, "Gas identification based on committee machine for microelectronic gas sensor," *IEEE Trans. Instrum. Meas.*, vol. 55, no. 5, pp. 1786–1793, Oct. 2006.
- [9] L. Zhang, F. Tian, H. Nie, L. Dang, G. Li, Q. Ye, *et al.*, "Classification of multiple indoor air contaminants by an electronic nose and a hybrid support vector machine," *Sensors Actuat. B, Chem.*, vol. 174, pp. 114–125, Nov. 2012.
- [10] K. Di Natale, A. Macagnano, E. Martinelli, R. Paolesse, G. D'Arcangelo, C. Roscioni, *et al.*, "Lung cancer identification by the analysis of breath by means of an array of non-selective gas sensors," *Biosensors Bioelectron.*, vol. 18, no. 10, pp. 1209–1218, 2003.
- [11] K. Polat and S. Gunes, "Computer aided medical diagnosis system based on principal component analysis and artificial immune recognition system classifier algorithm," *Expert Syst. Appl.*, vol. 34, no. 1, pp. 773–779, 2008.
- [12] K. Brudzewski, S. Osowski, and W. Pawlowski, "Metal oxide sensor array for detection of explosives at sub-parts-per million concentration levels by the differential electronic nose," *Sensors Actuat. B, Chem.*, vol. 161, no. 1, pp. 528–533, 2012.
- [13] A. P. Jones, "Indoor air quality and health," *Atmos. Environ.*, vol. 33, no. 28, pp. 4535–4564, 1999.
- [14] K. Sakai, D. Norbäck, Y. Mi, E. Shibata, M. Kamijima, T. Yamada, *et al.*, "A comparison of indoor air pollutants in Japan and Sweden: Formaldehyde, nitrogen, dioxide, and chlorinated volatile organic compounds," *Environ. Res.*, vol. 94, no. 1, pp. 75–85, 2004.
- [15] S. C. Lee and M. Chang, "Indoor and outdoor air quality investigation at schools in Hong Kong," *Chemosphere*, vol. 41, nos. 1–2, pp. 109–113, 2000.
- [16] M. Pardo and G. Sberveglieri, "Remarks on the use of multilayer perceptrons for the analysis of chemical sensor array data," *IEEE Sensors J.*, vol. 4, no. 3, pp. 355–363, Jun. 2004.
- [17] M. Pardo, G. Faglia, G. Sberveglieri, M. Corte, F. Masulli, and M. Riani, "A time delay neural network for estimation of gas concentrations in a mixture," *Sensors Actuat. B, Chem.*, vol. 65, no. 1, pp. 267–269, 2000.
- [18] L. Zhang, F. Tian, C. Kadri, G. Pei, H. Li, and L. Pan, "Gases concentration estimation using heuristics and bio-inspired optimization models for experimental chemical electronic nose," *Sensors Actuat. B, Chem.*, vol. 160, no. 1, pp. 760–770, 2011.
- [19] L. Zhang, F. Tian, S. Liu, H. Li, L. Pan, and C. Kadri, "Applications of adaptive Kalman filter coupled with multilayer perceptron for quantification purposes in electronic nose," *J. Comput. Inf. Syst.*, vol. 8, no. 1, pp. 275–282, 2012.
- [20] L. Zhang, F. Tian, S. Liu, J. Guo, B. Hu, Q. Ye, *et al.*, "Chaos based neural network optimization for concentration estimation of indoor air contaminants by an electronic nose," *Sensors Actuat. A, Phys.*, vol. 189, pp. 161–167, Jan. 2013.
- [21] D. Gao, M. Chen, and Y. Ji, "Simultaneous estimation of classes and concentrations of odors by an electronic nose using combinative and modular multilayer perceptrons," *Sensors Actuat. B, Chem.*, vol. 107, no. 2, pp. 773–781, 2005.
- [22] D. Gao, Z. Yang, C. Cai, and F. Liu, "Performance evaluation of multilayer perceptrons for discriminating and quantifying multiple kinds of odors with an electronic nose," *Neural Netw.*, vol. 33, pp. 204–215, Sep. 2012.
- [23] L. Zhang, F. Tian, X. Peng, L. Dang, G. Li, S. Liu, *et al.*, "Standardization of metal oxide sensor array using artificial neural networks through experimental design," *Sensors Actuat. B, Chem.*, vol. 177, pp. 947–955, Feb. 2013.
- [24] L. Zhang, F. Tian, S. Liu, L. Dang, X. Peng, and X. Yin, "Chaotic time series prediction of E-nose sensor drift in embedded phase space," *Sensors Actuat. B, Chem.*, vol. 182, pp. 71–79, Jun. 2013.
- [25] V. Maniezzo, "Genetic evolution of the topology and weight distribution of neural networks," *IEEE Trans. Neural Netw.*, vol. 5, no. 1, pp. 39–53, Jan. 1994.
- [26] J. Kennedy and R. C. Eberhart, "Particle swarm optimization," in *Proc. IEEE Int. Conf. Neural Netw.*, vol. 4, Nov./Dec. 1995, pp. 1942–1948.
- [27] R. C. Eberhart and Y. Shi, "Comparing inertia weights and constriction factors in particle swarm optimization," in *Proc. IEEE Evol. Comput.*, vol. 1, Jul. 2002, pp. 84–88.
- [28] J. Riget and J. S. Vesterstrom, "A diversity-guided particle swarm optimizer—the ARPSO," Dept. Comput. Sci., Univ. Aarhus, Aarhus, Denmark, Tech. Rep. 2002-02, 2002.
- [29] W. Jiang, Y. Zhang, and J. Xie, "A particle swarm optimization algorithm based on diffusion-repulsion and application to portfolio selection," in *Proc. IEEE Int. Symp. Inf. Sci. Eng.*, Dec. 2008, pp. 498–501.
- [30] B. Niu and Y. Zhu, "An improved particle swarm optimization based on bacterial chemotaxis," in *Proc. IEEE 6th WCICA*, vol. 1, Jun. 2006, pp. 3193–3197.
- [31] S. Wold, M. Sjöström, and L. Eriksson, "PLS-regression: A basic tool of chemometrics," *Chemometrics Intell. Lab. Syst.*, vol. 58, no. 2, pp. 109–130, Oct. 2001.
- [32] J. H. Sohn, M. Atzeni, L. Zeller, and G. Pioggia, "Characterisation of humidity dependence of a metal oxide semiconductor sensor array using partial least squares," *Sensors Actuat. B, Chem.*, vol. 131, no. 1, pp. 230–235, Apr. 2008.
- [33] T. Nes and H. Martens, "Principal component regression in NIR analysis: Viewpoints, background details and selection of components," *J. Chemometrics*, vol. 2, no. 2, pp. 155–167, Apr. 1988.
- [34] J. Getino, M. C. Horrillo, J. Gutiérrez, L. Arés, J. I. Robla, C. García, *et al.*, "Analysis of VOCs with a tin oxide sensor array," *Sensors Actuat. B, Chem.*, vol. 43, nos. 1–3, pp. 200–205, Sep. 1997.
- [35] T. Hagan, H. Demuth, and M. Beale, *Neural Network Design*. Boston, MA, USA: PWS-Kent, 1996.



machine learning.



**Lei Zhang** received the B.S. degree in electronic information engineering from the Nanyang Institute of Technology, China, in 2009, and the Ph.D. degree in circuits and systems from the College of Communication Engineering, Chongqing University, Chongqing, China, in 2013.

He was a Hong Kong Scholar in China in 2013. He is a Post-Doctoral Fellow with The Hong Kong Polytechnic University, Hong Kong. His current research interests include multisensor system, signal processing, pattern recognition, electronic nose, and

**Fengchun Tian** received the Ph.D. degree in electrical engineering from Chongqing University, Chongqing, China, in 1997.

He is currently a Full Professor with the College of Communication Engineering, Chongqing University. His current research interests include electronic nose technology, artificial olfactory systems, pattern recognition, chemical sensors, signal/image processing, wavelet, and computational intelligence. In 2006 and 2007, he was a part-time Professor with the University of Guelph, Guelph, ON, Canada.